Improving the Wind Energy Conversion System Dynamics during Fault Ride through: UPFC versus STATCOM

Mohammad Ferdosian
Electrical Engineering Department,
Islamic Azad University,
Kermanshah, Iran.
ferdosian_m@yahoo.com.

Hamdi Abdi
Electrical Engineering Department,
Razi University
Kermanshah, Iran.
hamdiabdi@razi.ac.ir

Ali Bazaei
Electrical Engineering Department,
University of Newcastle
Callaghan, NSW, Australia
ali.bazaei@newcastle.edu.au.

***Abstract*—There is a continuously growing demand for wind power generation capacity. This situation forces the revision of the grid codes requirements, to remain connected during grid faults, i.e., to ride through the faults, and contribute to system stability during fault condition. In a typical fault condition, the voltage at the Point of Common Coupling (PCC) drops below 80% immediately and the rotor speed of induction generators becomes unstable. In this paper, STATCOM and UPFC are used to improving the low voltage ride- through (LVRT) of wind energy conversion system (WECS) and to damp the rotor speed oscillations of induction generator under fault conditions. Furthermore, the performances of these two equipments are compared with each other. STATCOM can only recover voltage after fault clearing at the terminals of the wind energy conversion system (WECS), while controlling the UPFC as a virtual inductor can lead to increase the voltage at the WECS terminals during the fault clearing. The simulation results show that the UPFC is better than STATCOM in improving the LVRT and rotor stability of the WECS. Also, the simulation results show that UPFC can improve the voltage at the PCC in the fault period, with the voltage at the PCC easily recovering to 1pu, simultaneously. STATCOM can recover the voltage at the PCC only after the fault clearing with a high risk of decreasing the PCC voltage to zero during the fault.**

***Index Term*—Fixed Speed Wind Turbine (FSWT); Fault Ride Through (FRT), Unified Power Flow Controller (UPFC); Static Compensator (STATCOM); Wind Energy Conversion System (WECS); Induction Generator (IG)**

I. Introduction

Voltage control is one of the most important aspects in the interaction of wind turbine generation system (WTGS) to grid [1]. Coupling of WTGS to grid needs two main requirements: reactive power control during normal operating condition, and FRT capability during fault condition.

The FRT requirement ensures that wind turbine generators must remain connected to the grid in fault condition. To achieve the optimum efficiency in conversion from wind kinetic energy to the electrical energy, modern variable speed wind turbines (VSWT) are capable of varying their speed by power electronic converters. With an adequate control, the converters can be used to provide voltage support at the level of grid interface [2], [3].

However, modern VSWT are not the only ones installed in wind farms. There are important amounts of fixed speed wind turbine (FSWT) still in use. The FSWT exhibits poor FRT performance during fault condition as the induction generator draws reactive power during fault. When a fault occurs, a voltage drop suddenly occurs at the terminal of IG. Therefore, the electrical torque abruptly deceases to zero due to the reduced terminal IG voltage and the rotor speed starts to increase. After fault clearance, the reactive power consumption increases resulting in a period of voltage reduction at the IG terminal. Thus, the induction generator voltage does not recover immediately after the fault and a transient period follows. Therefore, the generator continues to accelerate and becomes unstable [4]–[6]. Hence, providing the required reactive power not only improves voltage regulation; but also helps to damp the rotor speed oscillations. Many papers have been discussed using of shunt FACTS controllers like SVC to improve the FRT of WECS [6]–[7].

In [8], Ahsanullah and Ravishankar described application of various dynamic controllers consisting of STATCOM and UPFC to enhance FRT in doubly-fed induction generators (DFIGs). Their study was mainly related to the effects of FACTS on the voltage variations at the point of common coupling (PCC) and FRT capability based on a fixed wind speed.

Application of a hybrid STATCOM (VSC + Capacitor Banks) for the regulation of the terminal voltage at PCC to the desired reference value was addressed by Moursi et al in [9]. The performance of the hybrid STATCOM was evaluated and analyzed with respect to full rating converter in view of the dynamic and transient operation of the three phase-to-ground fault.

In [10], Amjed and Lathika introduced an UPFC Controller in which the two converters and the capacitor are replaced with a dual-bridge matrix converter. Their main objective is directing ac to ac power conversion without DC energy storage links, resulting in a considerable decrease in UPFC's cost and volume. They employed Space Vector Pulse Width Modulation (SVPWM) control scheme to control the switching of the matrix converter.

978-1-4799-7800-7/15/$31.00 ©2015 IEEE

Effects of DFIG based wind energy conversion system with UPFC on power quality and harmonics were studied in [11, 12].

In [13], we demonstrated the capability of UPFC in improving the dynamic performance of WECS during a fault. However, the performance of STATCOM as a well-established FACT compensator has not been analyzed for WECS.

In this paper, STATCOM and UPFC are used for solving FRT problems of the interaction of wind energy conversion system (WECS) and power grid. As a supplementary work, we also compare the performances of UPFC and STATCOM in improving the WECS dynamics, under equal circumstances. The rest of this paper is organized as follow. In section II and III the STATCOM and UPFC basis are described. FSWT is illustrated in section IV. Effects of UPFC and STATCOM during fault and control strategy are presented in later sections, and finally the simulation results are presented in section VII.

II. STATCOM

The basic configuration of the STATCOM adopted in this work is shown in Fig. 1. The voltage-source converter (VSC) is the basic electronic part of a STATCOM, which converts the dc voltage into a set of three-phase output voltages with desired amplitude, frequency, and phase. Fig. 2 shows the V–I characteristic of STATCOM [14].

As shown in Fig. 2, the STATCOM can operate with its rated current even at reduced voltages. Hence, the injected reactive power varies linearly with the voltage. The effect of the STATCOM in this work is to inject reactive power into the grid when voltage drops as a result of a network short-circuit (fault).

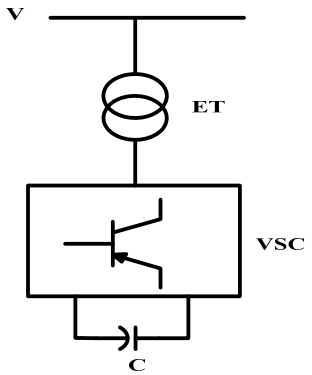

Fig. 1: Schematic diagram of basic STATCOM

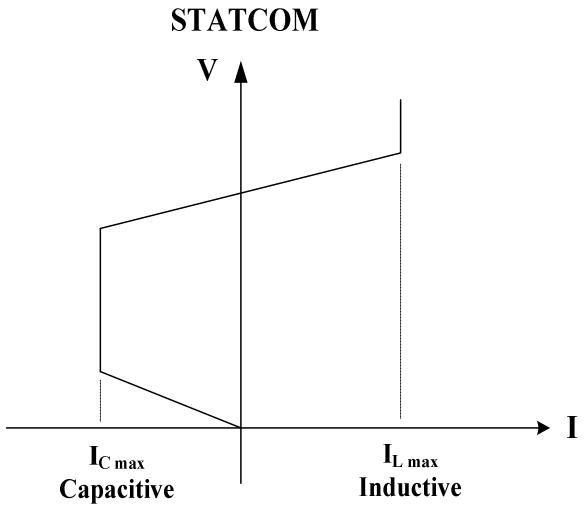

Fig. 2: V–I characteristics of STATCOM

III. Unified Power Flow Controller (UPFC)

Flexible AC Transmission Systems (FACTS) based power electronic converters like the UPFC are being used extensively in power Systems because of their ability to provide flexible power flow control [14, 20].

A schematic of the UPFC is shown in Fig. 3. It consists of two voltage source inverter (VSI). One is a shunt VSI and the other is series VSI. The shunt and series VSI are connected via a DC link, which includes a DC capacitor (C). The shunt converter of UPFC controls the connected UPFC bus and DC capacitor voltage [15]. The series converter of UPFC controls the line active and reactive power flow by injecting a series voltage of adjustable magnitude and phase angle.

Under steady state condition, series converter provides the main function of UPFC by injecting a voltage V_{pq} with controlled magnitude $(0<V_{pq}<V_{pqmax})$ and angle ρ, $(0<\rho<2\pi)$ in series with the transmission line, and controls power flow of the line. The phasor diagram of this mode is shown in Fig.4, where V_S represents sending end voltage, V_r receiving end voltage, V_{pq} is UPFC voltage, which is inserted in the power system through the series transformer, X is transmission line reactance and I is the line current [19].

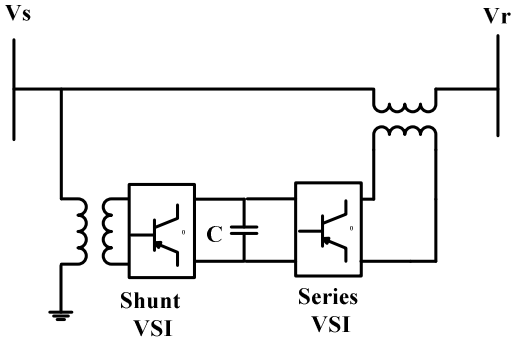

Fig. 3: UPFC schematic diagram

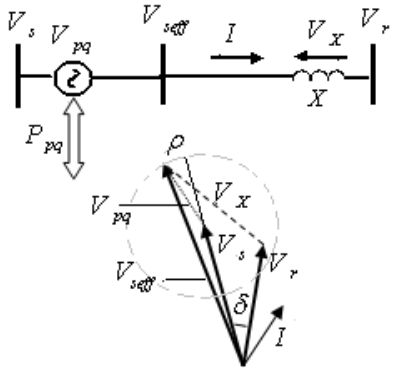

Fig. 4: Phase diagram of UPFC in normal condition. Effect of series inverter is only included as it is the dominant factor for the compensation of the voltage drop compared to the shunt inverter.

IV. Fixed Speed Wind Turbine

Fig. 5 shows the schematic diagram of a typical WECS. The wind speed model, the model of wind turbine, the mechanical model of the drive-train and induction generator are described in the following sections.

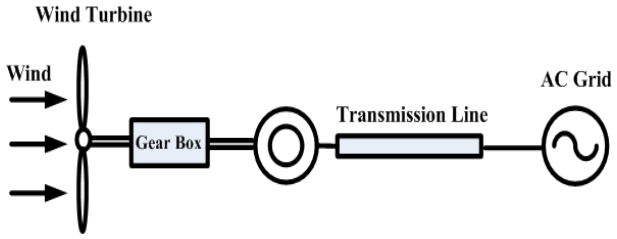

Fig. 5: Schematic diagram of typical WECS

A. *Wind Speed Model*

As shown in Fig. 6, wind speed is modeled as the sum of following components: Base wind speed, Gust wind speed, Ramp wind speed and Noise wind speed [18]. During the simulations, the steady component of the wind speed applied to the turbine is 15 m/s.

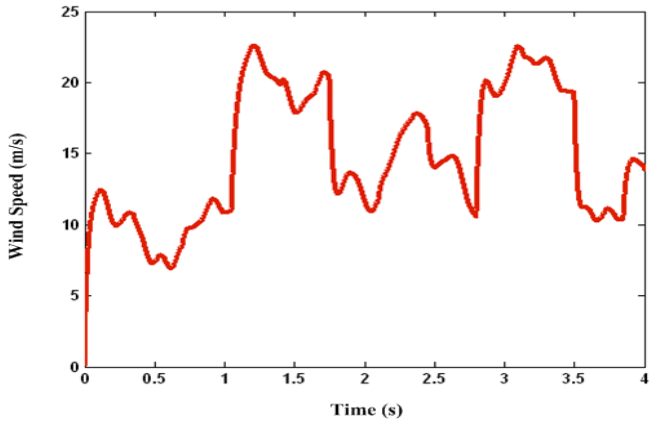

Fig. 6: Wind Speed Model

B. *Modeling Induction Generator*

The PSCAD/EMTDC software library provides a standard model for the induction generator, represented by a standard seventh-order model in a *d-q* reference frame [16]. This model is used in this paper.

C. *Wind Turbine Model*

In general, the relation between wind speed and mechanical power extracted from the wind can be described, as follow [12]-[13]:

$$P_{wt} = \frac{\rho}{2} A_{wt} C_p(\lambda,\theta) v_w^3 \qquad (1)$$

where, P_{wt} is the power extracted from the wind, ρ is the air density, V_w is the wind speed, C_p is the performance or power coefficient, λ is the tip speed ration, and A_{wt} is the area covered by the wind turbine rotor. Fig. 7 shows the C_p - λ curve. The performance coefficient is different for each turbine and is relative to the tip speed ratio λ and pitch angle β. In this paper, the C_p is selected as [18]:

$$C_P = \frac{1}{2}(\lambda - .022\beta^2 - 5.6)e^{-0.17\lambda} \qquad (2)$$

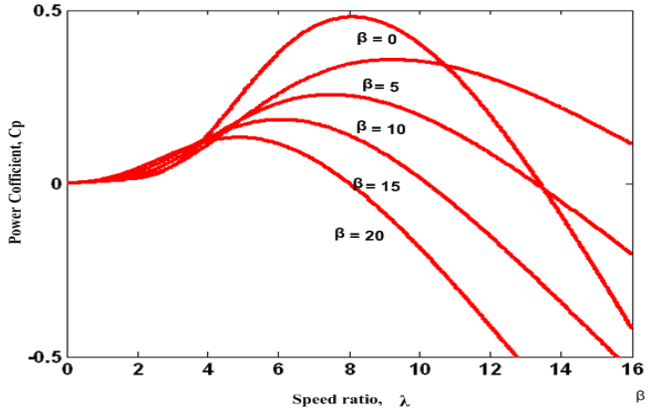

Fig. 7: CP- λ curves for different pitch angles

D. *Shaft model / drive train system*

The shaft model of the wind turbine is described by the two-mass model as shown in Fig. 8 and defined by the following equation [17-18]:

$$\frac{\partial \theta_s}{\partial t} = \omega_t - \omega_g \qquad (7)$$

$$T_t = J_t \frac{\partial \omega_t}{\partial t} - K_s \theta_s \qquad (8)$$

$$T_e = J_g \frac{\partial \omega_g}{\partial t} - K_s \theta_s \qquad (9)$$

where:

T_t: the mechanical torque referred to the generator side,
T_e: the electromagnetic torque,
J_t: the equivalent turbine-blade inertia,

J_g: the generator inertia,
ω_t: the turbine's rotational speed,
ω_g: the generator's rotational speed,
K: the shaft stiffness
θ_s: the angular displacement between the ends of the shaft

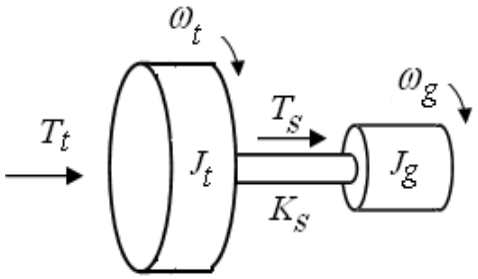

Fig. 8: Two mass model of wind turbine train

V. Effect of UPFC and STATCOM during Fault

During a downstream fault condition, large fault currents flow through the UPFC and STATCOM before the operation of the circuit breaker. This will cause the voltage at PCC to drop, which brings the shunt inverter of UPFC and STATCOM into operation. In this case, a protection system should disconnect the UPFC.

Furthermore, if not controlled properly, the UPFC and STATCOM might also contribute to this PCC voltage sag during the compensation process of the missing voltage, aggravating the fault situation. In this case, the electrical torque abruptly deceases to zero due to the voltage drop at the IG terminal and the rotor speed starts to increase [19]. During the fault, STATCOM cannot prevent the sudden dip in the voltage and the destabilizing electrical torque. Thus, it cannot restore the voltage at the PCC to the pre-fault level (1pu), after fault clearance. After clearing fault, the shunt inverter of STATCOM injects reactive power that helps to recover the voltage at the PCC.

UPFC acts as a large virtual inductance in series with the line. Controlling the UPFC as a virtual inductor also ensures zero real power absorption, minimizing the stress in the DC link during a fault. On the other hand, the UPFC aims to increase the voltage at the terminals of the WECS and thereby mitigates the destabilizing electrical torque and power during the fault. Also, the shunt inverter of UPFC injects reactive power after fault clearance, helping the recovery of PCC voltage.

VI. Control Strategy

A. *Shunt Converter Control Strategy*

The shunt converter of the UPFC and STATCOM controls the UPFC and STATCOM bus voltage/shunt reactive power and the dc link capacitor voltage [14]. In this case, the shunt converter voltage is decomposed into two components. One component is in-phase and the other is the magnitude of the UPFC and STATCOM bus voltage. De-coupled control system has been employed to achieve simultaneous control of the UPFC and STATCOM bus voltage and the dc link capacitor voltage as shown in Fig. 9.

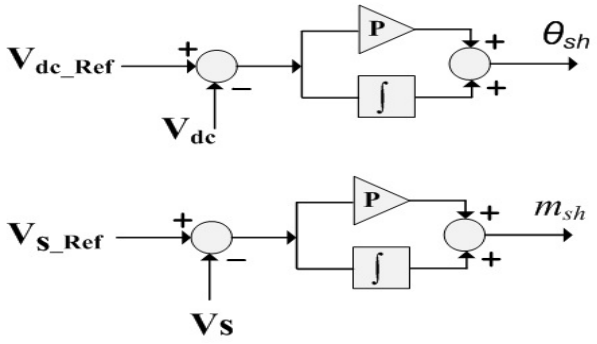

Fig. 9: UPFC and STATCOM shunt element control

B. *Series Converter Control Strategy*

The series converter of the UPFC provides simultaneous controls of real and reactive power flows in the transmission line [15]. To do so, the series converter injected voltage is decomposed into two components. One component of the series injected voltage is in quadrature and the other is in-phase with the UPFC bus voltage. The quadrature injected component controls the transmission line real power flow. This strategy is similar to that of a phase shifter. The in-phase component controls the transmission line reactive power flow as shown in Fig. 10.

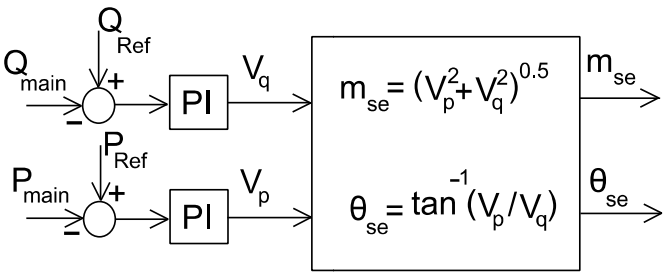

Fig. 10: UPFC series element control.

VII. Simulation Results

Single line diagrams of the simulated power system with UPFC and STATCOM are shown in Fig. 11 (a) and (b), respectively. The parameters of this system are listed in the appendix. A three phase short circuit fault is simulated in the middle of line 2, which starts at t=10s. After 0.4s, the circuit breaker isolated the faulted line. The simulations have been carried out with and without UPFC.

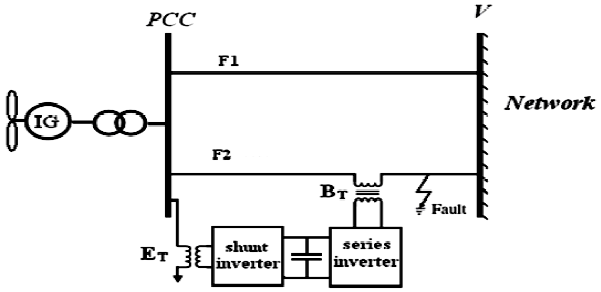

Fig. 11(case a): Simulated power system with UPFC

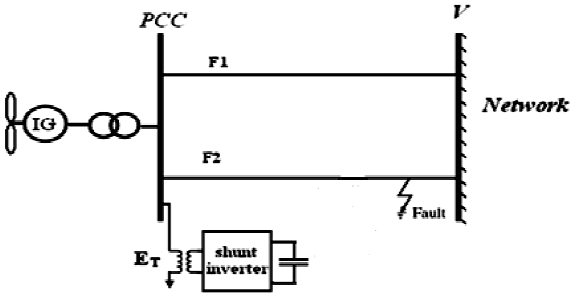

Fig. 11(case b): Simulated power system with STATCOM

Fig. 12 shows the rms value of the PCC voltage in the both cases, when using UPFC and STATCOM, individually. It is observed that when using STATCOM, the PCC voltage approximately decreases to zero and cannot be restored to the normal level (1 pu). The UPFC not only decreases the voltage sag to 0.4 pu, but also the voltage at PCC can be restored quickly after the fault by injecting reactive power after fault clearance through shunt inverter.

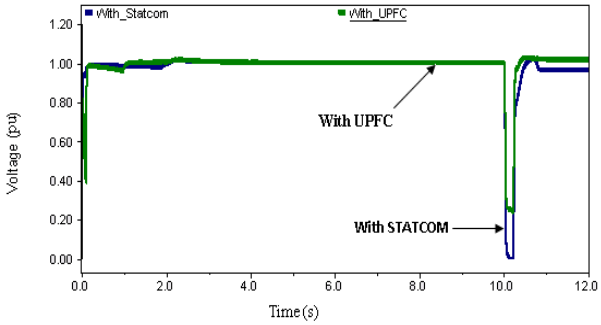

Fig. 12: Effect of UPFC and STATCOM on terminal voltage during fault

Figures 13 and 14 show the active and reactive power exchanged between the IG and the grid, respectively. During the fault, the UPFC prevents dropping the active power to zero thus after the fault clearing and the active power is restored to pre-fault level. However, when STATCOM is used, the active power during the fault interval is reduced to zero because of the voltage dip at the PCC. By using UPFC, the absorbing reactive power from the grid is significantly reduced, which helps to avoid other problems such as voltage collapse.

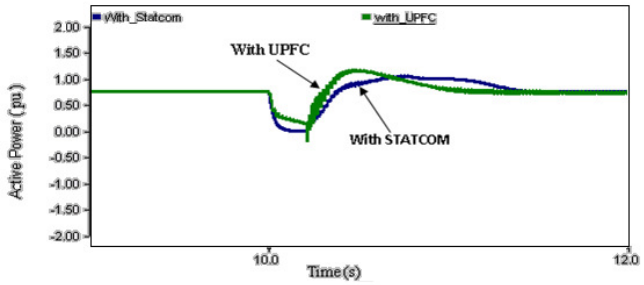

Fig. 13: Active power during fault

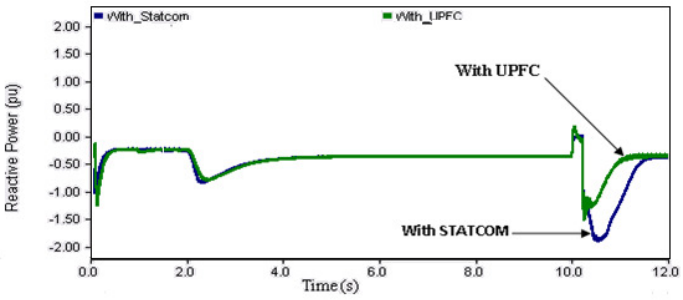

Fig. 14: Reactive power during fault

Figures 15 and 16 show the electrical torque and the rotor speed of the induction generator with STATCOM and UPFC, respectively. As shown in Fig. 15, with STATCOM the variation of the electrical torque is considerable because of the voltage dip at the PCC during the fault, thus, the rotor speed cannot be reduced to the pre-fault level as shown in Fig 16. When using UPFC, the variation of the electrical torque is reduced and is also restored at the pre-fault value. In addition, the rotor speed gradually reduces to the pre-fault level and the system is stable as shown in Fig.16.

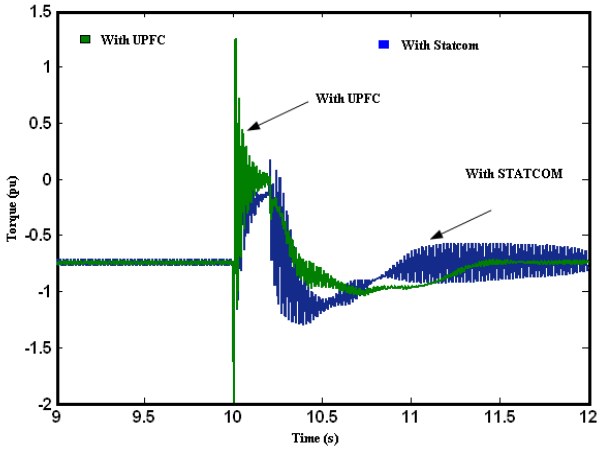

Fig. 15: Electrical torque of induction generator during fault

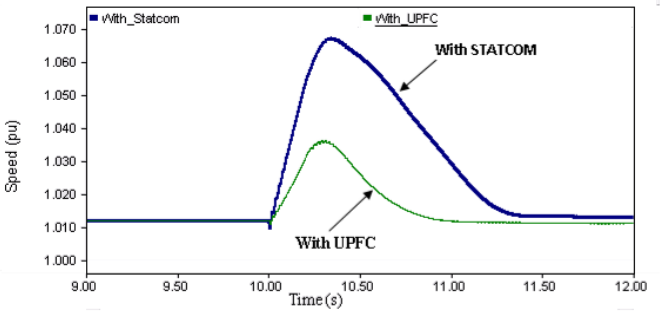

Fig. 16: Rotor speed of induction generator during fault

VIII. Conclusion

In this paper, effects of the STATCOM and UPFC on the performance of FSWT have been studied based on simulation by PSCAD/EMTDC. The simulation results show that the UPFC prevents the voltage dip during a fault and restores the

voltage after the fault clearance using a shunt inverter. In addition, it improves generator speed and the voltage stability of power grid integrated with WECS.

APPENDIX

GRID	
Supply	20 kV
Frequency	50Hz
Step down	69kV/20 kV
Transformer	10 MVA
X/R ratio	8

INDUCTION GENERATOR	
Power	500kW
Number of poles	4
Slip	1.8%
Power factor	0.9
Stator resistance	0.0577 Ω
Rotor resistance	0.0161 Ω
Stator reactance	0.0782 Ω
Rotor reactance	0.012 Ω
Magnetizing reactance	2.43 Ω

CONTROLLER PARAMETERS		K_P	K_I
SERIES INVERTER	ACTIVE POWER	5	0.2
	REACTIVE POWER	10	0.35
SHUNT INVERTER	DC LINK	1.5	100
	BUS VOLTAGE	3.5	0.1

REFERENCES

[1] J. F. Manwell, J. G. McGowan, and A. L. Rogers, "Wind Energy Explained: Theory, Design and Application", John Wiley & Sons Ltd, 2002.

[2] T. Ackermann, "Wind power in power systems" 1 ed., vol. 2. John Wiley & Sons Ltd, 2005, pp.742.

[3] T. Burton, D. Sharpe, N. Jenkins, and E. Bossanyi, "Wind energy handbook" John Wiley & Sons Ltd, Chichester, UK, 2001.

[4] J. M. Rodriguez and J. L. Fernandez, "Incidence on power system dynamics of high penetration of fixed speed and doubly fed wind energy systems: study of the Spanish case" IEEE Transactions on power system, Vol. 17, No. 4, 2002

[5] H. S. Ko, G. G. Yoon, and W. P. Hong, "Active use DFIG-based variable- speed wind-turbine for voltage control in power system operation,"J. Elect. Eng. Technol., Vol. 3, No. 2, pp. 254–262, Jun. 2008.

[6] S. M. Muyeen, M. A. Mannan, M. H. Ali, R. Takahashi, T. Murata, and J. Tamura, "Stabilization of wind turbine generator system by STATCOM" IEEJ Trans. Power Energy, Vol. 126, No. 10, Oct. 2006.

[7] M. Aten, J. Martinez, and P. J. Cartwright, "Fault recovery of a wind farm with fixed speed induction generators using a STATCOM" Wind Eng., Vol. 29, No. 4, PP. 365–375, 2005.

[8] K. Ahsanullah and J. Ravishankar. "Fault ride-through of doubly-fed induction generators." IEEE International Conference on Power, Signals, Controls and Computation (EPSCICON), 2012.

[9] M. El Moursi, Khaled Alobaidli, and H. H. Zeineldin. "A hybrid STATCOM for economical system installation with proven dynamic and transient response." 2013 IEEE PowerTech Conference (POWERTECH), Grenoble, France, June 2013.

[10] M. Amjed and B. S. Lathika. "Matrix converter based unified power flow controller." IEEE International Conference on Power, Signals, Control and Computations (EPSCICON), 2014.

[11] M. Rama Sekhara Reddy and M.Vijaya Kumar. "Power Quality Improvement in DFIG based Wind Energy Conversion System using UPFC." IOSR Journal of Engineering (IOSRJEN), vol. 3, no. 1, pp. 46-54, Jan. 2013.

[12] K. Ravichandrudu, P. Suman Pramod Kumar, and V.E. Sowjanya. "Mitigation of harmonics and power quality improvement for grid connected wind energy system using UPFC." International Journal of Application or Innovation in Engineering & Management (IJAIEM), vol. 2, no. 10, pp. 141-156, Oct. 2013.

[13] M. Ferdosian, H. Abdi, and A. Bazaei. "Improved dynamic performance of wind energy conversion system by UPFC." IEEE International Conference on Industrial Technology (ICIT), 2013.

[14] H. Gaztanaga, I. E. Otadui, D. Ocnasu, and S. Bacha, "Real-time analysis of the transient response improvement of fixed-speed wind farms by using a reduced-scale STATCOM prototype" IEEE Trans. Power Syst., Vol. 22, No. 2, PP. 658–666, May 2007.

[15] N. G. Hingorani, "High Power Electronics and Flexible AC Transmission System" IEEE Power Eng., pp. 3-4, Jul 1998.

[16] E. Gholipour, and S. Saadate. "Improving of Transient Stability of Power Systems Using UPFC" IEEE Trans. Power Deliv., Vol. 20, No. 2, pp 1677-1682, April 2005.

[17] A. Murdoch and R. S. Barton, "Control Design and Performance Analysis Of A 6 Mw Wind Turbine Generator" IEEE T Power Ap Syst, Vol. 102, No. 5, pp. 1340-1347, May 1983.

[18] P. M. Anderson and Anjan Bose, "Stability Simulation of Wind Turbine Systems" IEEE T Power Ap Syst, Vol. 102, No.12, pp. 3791-3795, Dec 1983.

[19] B. Adkins and R. G. Harley, "The General Theory of Alternating Current Machines" London, UK: Chapman & Hall, 1975.

[20] T. Yashaswini, G. P. Poornima, T.M Vasantha Kumara, and T. R. Narasimhegowda, "Grid Connected Wind Energy Conversion System Using Unified Power Flow Controller" International Journal of Science and Research, Volume 3, Issue 6, pp. 181-188, June 2014.